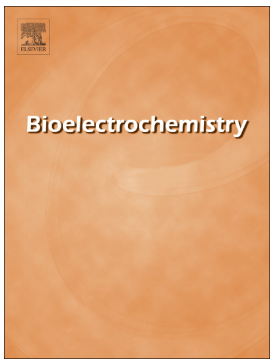

Gold nanoparticle-decorated reduced-graphene oxide targeting anti hepatitis B virus core antigen

Mohamad Farid Abd Muain, Kooi Hoong Cheo, Muhamad Nadzmi Omar, Amir Syahir Amir Hamzah, Hong Ngee Lim, Abu Bakar Salleh, Wen Siang Tan, Asilah Ahmad Tajudin

PII: S1567-5394(18)30042-2
DOI: doi:10.1016/j.bioelechem.2018.04.004
Reference: BIOJEC 7140

To appear in: *Bioelectrochemistry*

Received date: 24 January 2018
Revised date: 3 April 2018
Accepted date: 6 April 2018

Please cite this article as: Mohamad Farid Abd Muain, Kooi Hoong Cheo, Muhamad Nadzmi Omar, Amir Syahir Amir Hamzah, Hong Ngee Lim, Abu Bakar Salleh, Wen Siang Tan, Asilah Ahmad Tajudin , Gold nanoparticle-decorated reduced-graphene oxide targeting anti hepatitis B virus core antigen. The address for the corresponding author was captured as affiliation for all authors. Please check if appropriate. Biojec(2017), doi:10.1016/j.bioelechem.2018.04.004

Gold nanoparticle-decorated reduced-graphene oxide targeting anti hepatitis B virus core antigen

Mohamad Farid Abd Muain[a,c], Kooi Hoong Cheo[a,c], Muhamad Nadzmi Omar[a,c], , Amir Syahir Amir Hamzah[a,d], Hong Ngee Lim[b,e], Abu Bakar Salleh[a,d], Wen Siang Tan[c,f], Asilah Ahmad Tajudin[a,c*]

[a] Enzyme and Microbial Technology Research Centre, Universiti Putra Malaysia, 43400 UPM Serdang, Selangor Darul Ehsan, Malaysia
[b] Functional Device Laboratory, Institute of Advanced Technology, Universiti Putra Malaysia, 43400 UPM Serdang, Selangor Darul Ehsan, Malaysia
[c] Department of Microbiology, Faculty of Biotechnology and Biomolecular Sciences, Universiti Putra Malaysia, 43400 UPM Serdang, Selangor Darul Ehsan, Malaysia
[d] Department of Biochemistry, Faculty of Biotechnology and Biomolecular Sciences, Universiti Putra Malaysia, 43400 UPM Serdang, Selangor Darul Ehsan, Malaysia
[e] Department of Chemistry, Faculty of Science, Universiti Putra Malaysia, 43400 UPM Serdang, Selangor Darul Ehsan, Malaysia
[f] Institute of Bioscience, Universiti Putra Malaysia, 43400 UPM Serdang, Selangor Darul Ehsan, Malaysia

*Corresponding author. Tel: +603 8946 7241
Email address: asilah_at@upm.edu.my (Ahmad Tajudin, A.)

Highlights

- Protein-functionalized graphene-based nanocomposite to sense anti-HBcAg
- Limit of detection of 3.80 ng mL^{-1} in spiked samples
- Protein-functionalized electrode is selective and specific towards anti-HBcAg
- Works on diluted human serum sample

Abstract

Hepatitis B virus core antigen (HBcAg) is the major structural protein of hepatitis B virus (HBV). The presence of anti-HBcAg antibody in a blood serum indicates that a person has been exposed to HBV. This study demonstrated that the immobilization of HBcAg onto the gold nanoparticles-decorated reduced graphene oxide (rGO-en-AuNPs) nanocomposite could be used as an antigen-functionalized surface to sense the presence of anti-HBcAg. The modified rGO-en-AuNPs/HBcAg was then allowed to undergo impedimetric detection of anti-HBcAg with anti-estradiol antibody and bovine serum albumin as the interferences. Upon successful detection of anti-HBcAg in spiked buffer samples, impedimetric detection of the antibody was then further carried out in spiked human serum samples. The electrochemical response showed a linear relationship between electron transfer resistance and the concentration of anti-HBcAg ranging from 3.91 ng mL^{-1} to 125.00 ng mL^{-1} with lowest limit of detection (LOD) of 3.80 ng mL^{-1} at 3 σ m^{-1}. This established method exhibits potential as a fast and convenient way to detect anti-HBcAg.

Keywords: Hepatitis B virus, antibody, impedimetric biosensor, reduced graphene oxide, gold nanoparticles

1. Introduction

Hepatitis B virus (HBV) can be transmitted by direct contact with exposure to infected blood and other body fluids including saliva, sweat, semen and breast milk [1]. Human become the natural host of this deadly virus, in which the viral replication takes place in the liver. The virion is enveloped by a lipid membrane containing three different forms of hepatitis B surface antigen (HBsAg) [2]. Inside the envelop is the viral capsid which is made from many copies of hepatitis B core antigen (HBcAg). The capsid encapsidates a partially double stranded DNA genome and the DNA polymerase containing reverse transcription activity [3].

In an acute infection, serological markers which include HBsAg and anti-HBcAg develop in the patient's blood. If the patient successfully recover, HBsAg will disappear from the blood, and the production of anti-HBsAg serves as an indicator of immunity towards the viral infection [4]. Unfortunately, about 5-10 % of healthy adults, 50 % of young children, and 90% infants failed to develop immunity towards HBV infection, and will result in the development of chronic infection. For this type of infection, HBsAg and anti-HBcAg will be present in the blood and can remain from six to seven months up to a lifetime [3]. Unlike acute infection, chronic HBV-infected patients will not be able to produce anti-HBsAg even after recovery [4], and they are likely to develop cirrhosis and hepatocellular carcinoma [4,5]. Another type of HBV infection is called occult infection which is characterized by the presence of viral HBV DNA with the absence of HBsAg in a patient's blood [6].

Detection of HBsAg in infected blood samples by enzyme-linked immunosorbent assay (ELISA), and polymerase chain reaction (PCR) amplification of viral DNA are commonly being used to detect the presence of HBV [6]. However, these methods are insufficient as a single test for occult HBV patients as they possess HBV DNA but with no detectable HBsAg in their blood. In the case of HBsAg being the first screening test for HBV infection, a second PCR test on HBV DNA may still need to be carried out, or the transmission of virus to healthy person via blood transfusions or liver transplantation from infected patients with negative HBsAg but possessing anti-HBcAg may occur [7]. An ultra-sensitive PCR amplification with limit of detection of 10 copies of the viral DNA for each reaction, despite being costly and time consuming, may be the only option for detecting HBV infection in occult HBV patients [8]. Therefore, the development of integrated systems for rapid, highly sensitive simultaneous detection of a comprehensive panel of serological markers for HBV infection is imperative.

One of the immune responses by the body after the HBV infection is the production of immunoglobulin (Ig) classes G and M against the HBcAg [9]. IgG-anti-HBcAg will remain in the patient's blood for a lifetime, whereas IgM-anti-HBcAg will decline until it becomes undetectable after the recovery from the infection [10]. Sensing for the presence of anti-HBcAg IgG in individuals may provide a promising solution due to its prevalence as a viral marker and may be essential in HBV endemic countries, since it is the best serological marker to detect patients who have been exposed to the virus at

any time in their lives [10,11]. It is also crucial to have a HBV screening which is time-efficient and is portable for a faster and better screening against HBV-contaminated blood in worldwide blood banks, thus decreasing the transmission of the virus through blood transfusions [11]. Detection of anti-HBcAg through ELISA had been described previously in the literature [12], but unfortunately, performing ELISA in low-resource settings is limited by long incubation time, the need for large volumes of precious reagents, and also well-equipped laboratories.

Enormous advancements have been achieved in the development of electrochemical immunosensors to be applied in various fields including agriculture, environmental and industrial monitoring, safety of foods, biomedicine, and quality control, development and screening of drugs, forensic analysis, prevention and control of epidemic diseases as well as point of care diagnostics, and the main challenge faced by these methods is achieving the lowest limit of detection [13–15]. Various strategies and architectures of electrochemical immunosensors, which include enzyme-labelled immunosensors[16], metal nanoparticle- and quantum dot-labelled immunosensors [17,18], capacitive [19] and impedimetric immunosensor [20], and magnetoimmunosensors [21] have been proposed [14]. Nanostructures such as graphene oxide (GO), reduced graphene oxide (rGO), carbon nanotubes and nonporous materials have enticed great interest among researchers due to their excellent properties including are biocompatibility, electrically conductive, cost-effective and ease of fabrication [22]. Recently, electrochemical detection of anti-HBcAg by the means of high sensitivity electrochemical detection which employed carbon nanotube as the antigen-functionalized surface had been proposed with the LOD of 0.03 ng ml^{-1} [11].

As aforementioned, one of the nanostructures that can be used as the antigen-functionalized surface is rGO due to its comparable characteristics with pristine graphene sheets. These characteristics include two-dimensional carbon nanostructure that possess high intrinsic mobility which allow faster charge transfer [23]. This rGO nanostructure can be fabricated from GO by reducing it chemically and it has better electrical conductivity compared to GO itself [24]. In terms of its application as a functionalized base for the development of biosensor, rGO has been demonstrated as a good platform for enzymes [25], DNA [26], metallic oxides [27], metallic nanoparticles [28] and quantum dots [29]. Herein, this study demonstrated the combination of immunoaffinity and electrochemical concepts in order to detect anti-HBcAg via HBcAg-immobilized gold nanoparticles-decorated rGO (rGO-en-AuNPs) nanocomposite as a promising way to develop an anti-HBcAg biosensor with simple design, yet having high sensitivity and specificity, also faster response, with minimal interferences.

2. Materials and Methods

2.1 Materials

Graphite powder was obtained from Ashbury Graphite Mills Inc. (New Jersey, USA). Chloroauric acid ($HAuCl.3H_2O$) was purchased from Sigma-Aldrich (Missouri, USA). Ethanol (95%) was purchased from Systerm (Malaysia). Phosphate buffered

solution (PBS) was prepared by mixing the stock solution of disodium hydrogen phosphate (Na_2HPO_4, 99%) and sodium dihydrogen phosphate (NaH_2PO_4, 99%); powder purchased from Friendemann Schmidt Chemical (Australia). Mouse anti-HBcAg monoclonal IgG and anti-estradiol were purchased from Santa Cruz Biotechnology Inc (Texas, USA) and Abcam (Cambridge, UK) respectively. Bovine serum albumin (BSA) was obtained from Novagen, EMD Bioscience Inc (California, USA). Screen-printed electrode (SPE) DRP-C110 was obtained from Dropsens (Parque Technologico de Autorias, Spain). Other chemicals used in this study were of analytical grade and used as received without further purification. All solutions were prepared using deionized water (dH_2O) synthesized by Milli-Q Merck Millipore (Massachusets, USA) water purification system.

2.2 Instrumentation

All cyclic voltammetry (CV) and electrochemical impedance spectroscopy (EIS) analyses were carried out using the Princeton VersaSTAT 3 (Ametek Scientific Instruments, Pennsylvania, USA) potentiostat that was controlled by the VersaStudio version 2.52 (Ametek Scientific Instruments, Pennsylvania, USA) as the computer interface.

2.3 Synthesis of rGO-en-AuNPs nanocomposite

The rGO was originated from graphene oxide(GO) that was earlier fabricated through simplified Hummer's method as previously described [30], where 3 ml of 9.48 mg ml^{-1} GO was allowed to be reduced by 25 ml of 0.1 M ethylenediamine by refluxing for 3 hours at temperature of 70 °C by stirring. Then, 3 ml of 0.1 % (w/v) $HAuCl_4.3H_2O$ was added to the previous mixture and further be refluxed for 30 minutes at the same temperature with continuous stirring. Next, 6 ml of 1 % w/v sodium citrate was added drop wise in to the reaction system and allowed for further refluxing for 30 minutes at the same temperature. Final reflux solution was cooled down and centrifuged twice at 4000 rpm for 10 minutes and be washed with dH_2O for several times. In order to produce a homogenous solution, 20 ml of dH_2O was added to the precipitate layer and was ultrasonicated for 1 hour. The process of fabricating rGO-en-AuNPs nanocomposite was based on the reduction of two oxygen-containing functional groups (epoxy and carboxyl groups) of original GO by ethylenediamine through refluxing process, which then coupled electrostatically with chloroauric anion ($AuCl_4^-$) with protonated amino groups of ethylenediamine. Then, $AuCl_4^-$ was reduced to gold nanoparticles (AuNPs) by sodium citrate as reducing agent.

2.4 Preparation of rGO-en-AuNPs-functionalized SPE

The surface of SPE was rinsed twice with dH_2O and allowed to be air dried. About 1 ml of the homogenous nanocomposite was mixed with 3 ml of dimethylformamide (DMF) and ultrasonicated for 15 minutes to produce a homogenous

suspension. About 10 µl of the latter was drop casted on the surface of working electrode of SPE (SPE/rGO-en-AuNPs), and air dried to evaporate and eventually to remove the DMF.

2.5 Preparation of HBcAg-functionalized electrode

Escherichia coli harbouring plasmid pR1-11E was used in the production of the recombinant HBcAg as described previously [31]. The purified HBcAg (500 ng of HBcAg in 50 mM PBS) was immobilized on SPE/rGO-en-AuNPs. The electrode was incubated at 4 °C for 15 hours. After the incubation, the electrode was rinsed with 5 ml of dH_2O and the resulting solution was tested using the Bradford assay [32] to determine the percentage of HBcAg immobilized on the nanocomposites. Then, the electrode was incubated with 3 % BSA to block free and empty spaces for protein binding. The electrode at this stage is referred as SPE/rGO-en-AuNPs/HBcAg/BSA. Characterization of this electrode was done by running CV analysis at the scan rate of 50 mV in the potential window of -1.0 V to 1.0 V, and EIS with the sweep frequency from 100 kHz to 0.01 Hz and amplitude of 5 mV RMS in electrolyte solution comprises of 5 mM potassium hexacyanoferrate ($K_3Fe(CN)_6$) as redox probe and 0.1 M potassium chloride (KCl) as supporting electrolyte. The integrated Ag electrode on the SPE was used as the reference electrode.

2.6 Sensing of anti-HBcAg in spiked buffer samples

Adapting from previous study [33], the anti-HBcAg detection was carried out with five different concentrations ranging from 3.91 ng mL^{-1} to 125.00 ng mL^{-1} that were prepared in 50 mM PBS and incubated on SPE/rGO-en-AuNPs/HBcAg/BSA separately, at 4 °C for two hours. Finally, each electrode was subjected for EIS analyses by using a potentiostat with the sweep frequency from 100 kHz to 0.01 Hz and amplitude of 5 mV RMS in electrolyte solution comprises of 5 mM $K_3Fe(CN)_6$ as redox probe and 0.1 M KCl as supporting electrolyte.

2.7 Specificity study

A non-related antibody, anti-estradiol at the concentration ranging from 3.91 ng mL^{-1} to 125.00 ng mL^{-1} was incubated separately on SPE/rGO-en-AuNPs/HBcAg/BSA at 4 °C for two hours. Then, EIS analyses were carried out as described above.

2.8 Selectivity study

Adapting from previous study [34], the prepared SPE/rGO-en-AuNPs/HBcAg/BSA was reacted in a mixed solution containing anti-HBcAg and anti-estradiol of the same concentration ranging from 3.91 ng mL^{-1} to 125.00 ng mL^{-1}, and 100 ng mL^{-1} BSA in 50 mM PBS. Incubation lasted for two hours at 4 °C. Then, EIS analyses were carried out as described above.

2.9 Detection of anti-HBcAg in human serum samples

The prepared SPE/rGO-en-AuNPs/HBcAg/BSA was allowed to be reacted in 1:1000 diluted human serum samples containing anti-HBcAg with concentration ranging from 3.91 ng mL^{-1} to 125.00 ng mL^{-1}. Incubation lasted for two hours at 4 °C. Then, EIS analyses were carried out as described above.

3. Results and Discussions

3.1 Antigen functionalization and characterization of electrode

Addition of the nanocomposite onto the working electrode surface of SPE enhanced the conductivity and the electroactive areas of the system [30,35] and decrement of conductivity upon addition of biomolecules, HBcAg and BSA, can be seen due to the obstruction of electron transfer flow of $Fe(CN_6)^{-3/-4}$ through the electrolyte [34]. The latter changes of electrical properties of the electrode also can be seen as the increment of resistivity which confirmed the existence of biomolecules on the nanocomposite or they had successfully been immobilized on the nanocomposite [36]. Electrochemical analysis by means of CV and EIS had been carried out to characterize the SPE/rGO-en-AuNPs/HBcAg/BSA (Figure 1).

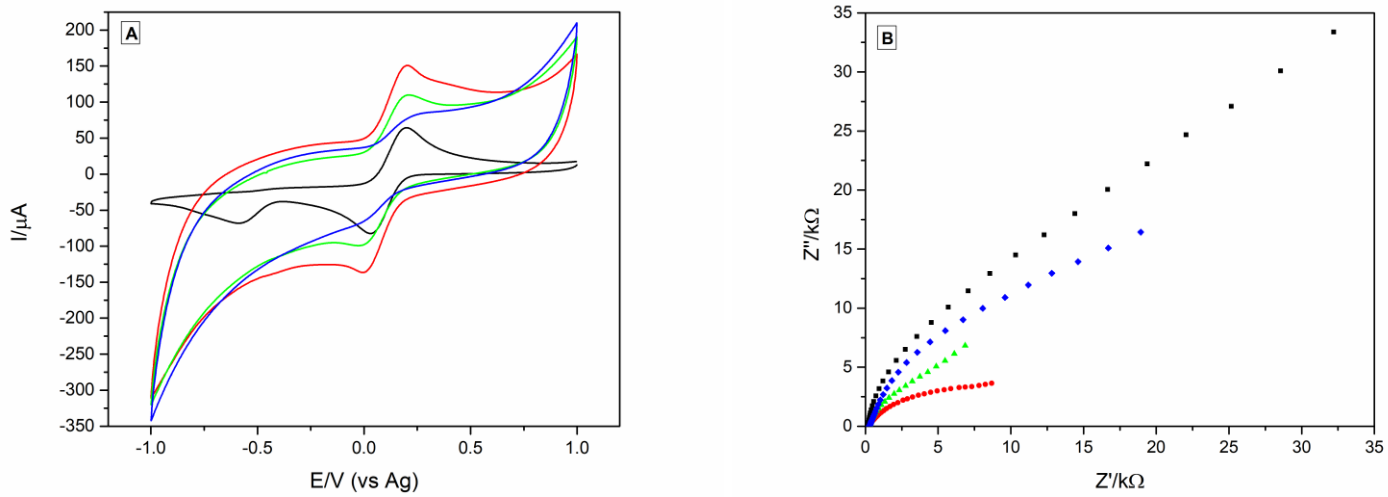

Figure 1: HBcAg-functionalized SPE characterization. CV characterization in 5 mM $K_3Fe(CN_6)$ and 0.1 M KCl (A), Nyquist plot of EIS characterization in 5 mM $K_3Fe(CN_6)$ and 0.1 M KCl (B). bare SPE (CV: black line; EIS: black square), SPE/rGO-en-AuNPs (CV: red line; EIS: red circle), SPE/rGO-en-AuNPs/HBcAg (CV: green line; EIS: green triangle), and SPE/rGO-en-AuNPs/HBcAg/BSA (CV: blue line; EIS: blue diamond).

Figure 1(A) shows the cyclic voltammogram profiles of HBcAg-functionalized electrode. Upon modification with the nanocomposites, the cathodic and anodic peaks increased greatly for about 175.91 % and 66.25 % respectively after bare SPE was modified using the nanocomposites due to the enhancement of conductivity by the nanocomposite [35]. After the immobilization of HBcAg, the cathodic and anodic peaks were reduced for about 27.15 % and 24.81 % respectively, and both of the peaks further reduced for about 27.37 % and 36.71 % respectively after the free and empty spaces of nanocomposites for protein binding had been blocked with BSA. Decrement of those peaks was due to the formation of insulation layer by the protein on the surface of nanocomposite which reduced the electron transfer flow between electrode and electrolyte [34].

EIS analysis investigates the electron transfer that occur between electrode and the electrolyte. Its profile commonly comprises two main parts which are the high frequency part (semi-circular shaped) and the low frequency part (linear shaped). The diameter of semi-circular shaped depicts the R_{ct} of the electrode, while the linear part relates to the diffusion of electron transfer process [30]. Figure 1(B) shows the Nyquist plot of electrode functionalization by HBcAg in terms of resistivity that is on par with the CV profiles. Upon modification of electrode with the nanocomposite, the R_{ct} of the electrode decreased tremendously from 40.41 kΩ for bare SPE to 9.93 kΩ for nanocomposite-modified SPE (SPE/rGO-en-AuNPs) indicating that the nanocomposite enhanced the conductivity and electron transfer between the $Fe(CN_6)^{-3/-4}$ and the electrode [30]. Previously, this fabricated nanocomposite had shown better conductivity when compared to unreduced graphene oxide, and the AuNPs was proven to accelerate the electron transfer process [30]. After the immobilization of HBcAg on top of the nanocomposite, R_{ct} showing an increment to 12.32 kΩ, and further increase to 30.95 kΩ after the application of BSA due to obstruction of the electron flow by the biomolecule [34]. It is crucial to apply BSA as to prevent non-specific binding of the biomolecule of interest to the nanocomposite [37] which will give a false positive result of bioreceptor recognition. Through both CV and EIS characterizations, it was found that the electrode was successfully functionalized by HBcAg.

HBcAg protein was immobilized on the nanocomposites by attachment to AuNPs via weak metal-protein interactions [38] with no application of crosslinkers and labels. This will reduce time for the protein to bind to the nanocomposites as additional time is needed for the application of crosslinkers. Furthermore, laborious step of using labels and expensive instruments can be avoided [39] just to confirm the immobilization of the antigen. Through the Bradford assay [32], it was found that approximately 86.00 % HBcAg was successfully immobilized on the nanocomposite.

3.2 Impedimetric detection of anti-HBcAg

Figure 2(A) shows the impedimetric spectra of proposed immunosensor in 5 mM $K_3Fe(CN_6)$ and 0.1 M KCl after the incubation of HBcAg-functionalized electrode with different concentrations of anti-HBcAg for two hours. As expected, the R_{ct} increases

along the increment of concentration of anti-HBcAg. The corresponding calibration curve (Figure 2(B)) clearly indicates the linearity relationship of both measured R_{ct} and the concentration of anti-HBcAg over a range of 3.91 ng mL^{-1} to 125.00 ng mL^{-1} with a linear regression equation of ΔR_{ct} = 0.0261[anti-HBcAg] + 6.421 and regression coefficient of 0.982. The increment of the resistivity was due to the electrically insulating nature of protein which hindered the electron transfer flow [11] after the immunocomplex formation between HBcAg and anti-HBcAg.

The proposed method of this immunosensor exhibit LOD of 3.80 ng mL^{-1} (at 3 σ m^{-1}), while the clinically significant level of anti-HBcAg is around 2.00 ng mL^{-1} to 5.00 ng mL^{-1} [11]. This indicates the immunosensor has a few advantages over previously reported sensor. The advantages include simplicity in terms of preparing the HBcAg-functionalized surface without any chemical modification using crosslinkers prior to bioreceptor immobilization and a laborious setup of a conventional three-electrode system can also be avoided.

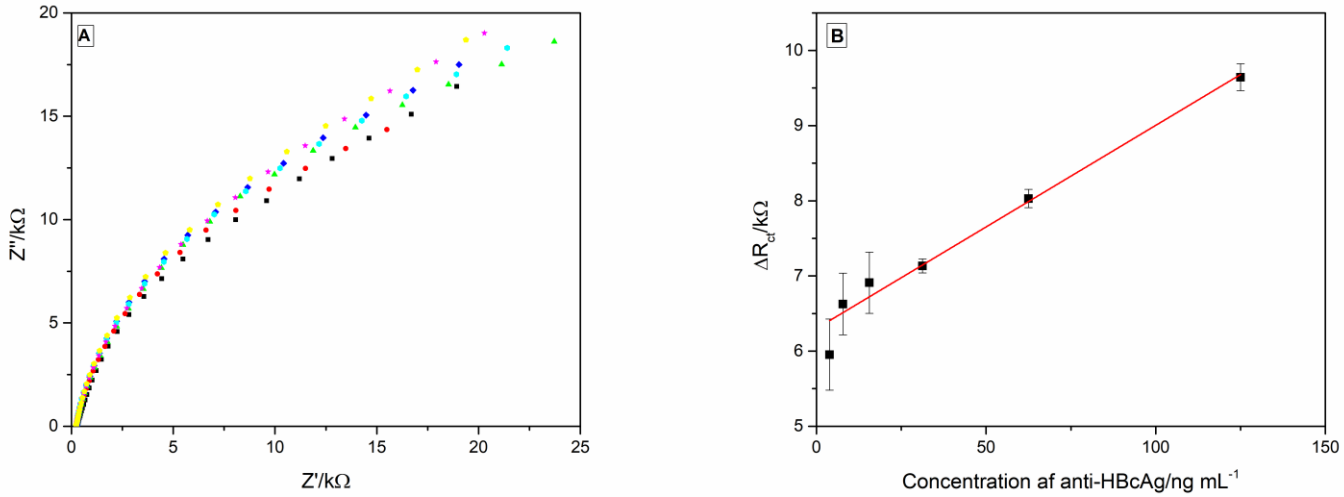

Figure 2: Impedimetric detection of anti-HBcAg. Nyquist plot of impedimetric analysis in 5 mM $K_3Fe(CN_6)$ and 0.1 M KCl (A), calibration curve showing relationship of ΔR_{ct} (changes in resistance after immunocomplex formation) and the varying concentration of anti-HBcAg incubated on HBcAg-functionalized electrode (B). HBcAg-functionalized SPE (black square), and HBcAg-functionalized SPE that was incubated with anti-HBcAg with the concentration of 3.91 ng mL^{-1} (red circle), 7.81 ng mL^{-1} (green triangle), 15.63 ng mL^{-1} (blue diamond), 31.25 ng mL^{-1} (cyan hexagon), 62.50 ng mL^{-1} (magenta star), 125.00 ng mL^{-1} (yellow pentagon).

3.3 Specificity of the immunosensor

Evaluation of the proposed immunosensor in terms of specificity of the immobilized HBcAg as the bioreceptor towards the anti-HBcAg was done by reacting the HBcAg-functionalized electrode with a non-related antibody. Interestingly, there was no apparent increment of R_{ct} even when the concentration of anti-estradiol was increased up to 125.00 ng mL^{-1} (Figure 3). These denote that the HBcAg epitope specifically formed the immunocomplex with the paratope of the anti-HBcAg, indicating high immunospecificity of the immunosensor towards anti-HBcAg with no apparent cross-reaction with the non-related antibody tested. In addition, this study also confirmed that the HBcAg-functionalized electrode was successfully blocked by BSA as there was no increment of R_{ct} which could have occurred, should there be an unspecific binding of anti-estradiol to the nanocomposite.

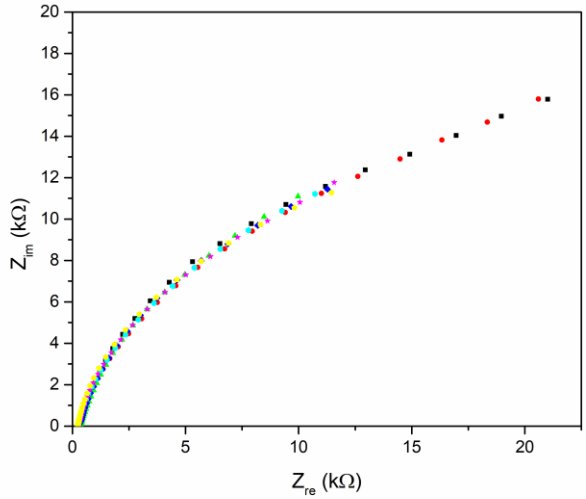

Figure 3: Nyquist plot of impedimetric study of HBcAg-functionalized electrode with anti-estradiol in 5 mM $K_3Fe(CN_6)$ and 0.1 M KCl. HBcAg-functionalized SPE (black square), and HBcAg-functionalized SPE that was incubated with anti-estradiol with the concentration of 3.91 ng mL^{-1} (red circle), 7.81 ng mL^{-1} (green triangle), 15.63 ng mL^{-1} (blue diamond), 31.25 ng mL^{-1} (cyan hexagon), 62.50 ng mL^{-1} (magenta star), 125.00 ng mL^{-1} (yellow pentagon).

3.4 Selectivity of the immunosensor

In order to evaluate the selectivity of this anti-HBcAg detection by the HBcAg-functionalized electrode in an environment with an increased complexity, interferences were introduced to the system in which the detection of anti-HBcAg was carried out in a mixed solution consisting of anti-HBcAg and anti-estradiol of the same concentration, and 100 ng mL^{-1} BSA in 50 mM PBS. This testing was then compared with the detection of anti-HBcAg in a pure anti-HBcAg solution.

Figure 4 (A) shows the impedimetric spectra of proposed immunosensor in 5 mM $K_3Fe(CN_6)$ and 0.1 M KCl after the incubation of HBcAg-functionalized electrode in the mixed solution of antibodies and BSA for two hours. As expected, the R_{ct} increases along the increment of concentration of anti-HBcAg in a mixed solution. The corresponding calibration curve (Figure 4(B)) clearly indicates the linearity relationship of both measured R_{ct} and the concentration of anti-HBcAg over a range of 3.91 ng mL^{-1} to 125.00 ng mL^{-1} with a linear regression equation of ΔR_{ct} = 0.0315[anti-HBcAg] + 6.309 and regression coefficient of 0.971.

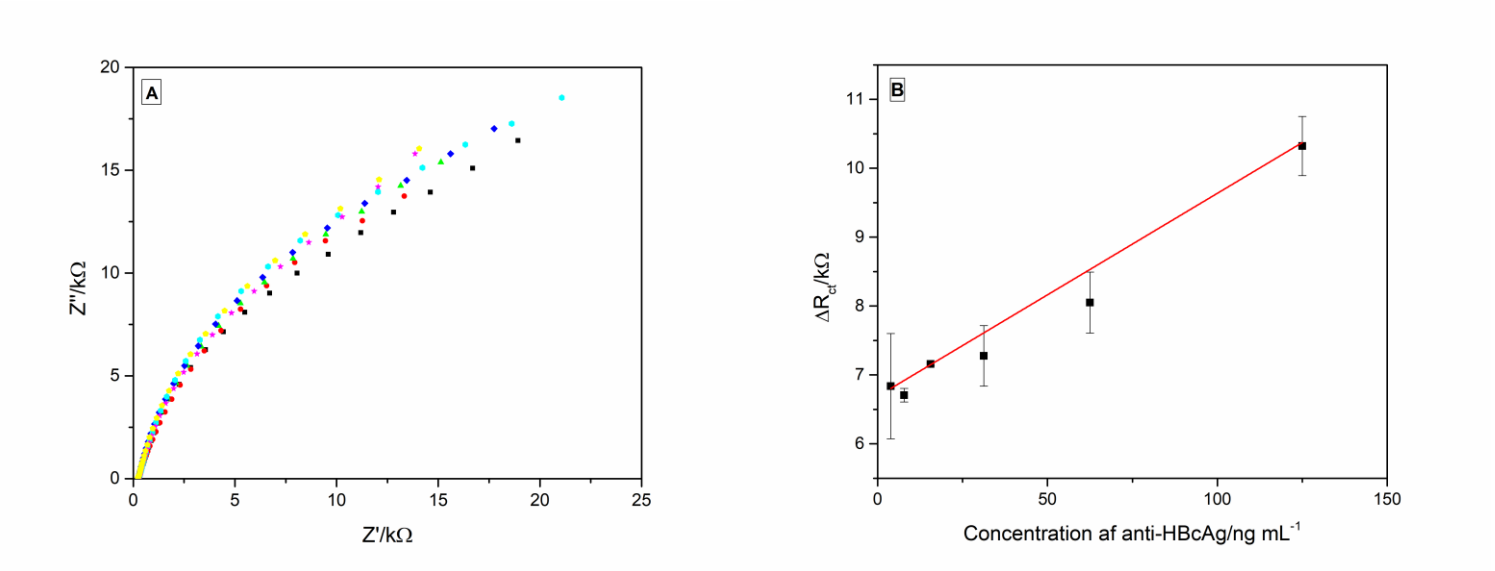

Figure 4: Impedimetric profile of HBcAg-functionalized electrode showing the detection of anti-HBcAg from a mixed solution. Nyquist plot of impedimetric analysis in 5 mM $K_3Fe(CN_6)$ and 0.1 M KCl (A), calibration curve showing relationship of ΔR_{ct} (changes in resistance after immunocomplex formation) and the varying concentration of anti-HBcAg in mixed solution incubated on HBcAg-functionalized electrode (B). HBcAg-functionalized SPE (black square), and HBcAg-functionalized SPE that was incubated with mixed protein solution containing anti-HBcAg with the concentration of 3.91 ng mL^{-1} (red circle), 7.81 ng mL^{-1} (green triangle), 15.63 ng mL^{-1} (blue diamond), 31.25 ng mL^{-1} (cyan hexagon), 62.50 ng mL^{-1} (magenta star), 125.00 ng mL^{-1} (yellow pentagon).

Through this selectivity study, it was found that the immunosensor is able to detect the anti-HBcAg within the concentration of 3.91 ng mL^{-1} to 125.00 ng mL-1, with LOD of 3.88 ng mL^{-1} at 3 σ m^{-1}. The variation of of R_{ct} produced by detection of pure anti-HBcAg (as in 3.2 Impedimetric detection of anti-HBcAg) and anti-HBcAg in mixed solution can be compared by calculating the relative standard deviation (RSD) to see the accurateness and precision of R_{ct} produced by detection of anti-HBcAg in mixed solution. It was found that RSD values to be 1.68 %, 0.85 %, 2.48 %, 1.41 %, 0.18 % and 4.82 % for the comparison between 3.91 ng mL^{-1}, 7.81 ng mL^{-1}, 15.63 ng mL^{-1}, 31.25 ng mL^{-1}, 62.50 ng mL^{-1}, and 125.00 ng mL^{-1} of pure and mixed solutions of anti-HBcAg. After successful blocking of free and empty spaces of the nanocomposite by 3 % BSA, no immunocomplex formation towards anti-estradiol as in the specificity study, and also lower RSD value, this demonstrates that anti-HBcAg was detected efficiently by HBcAg-functionalized electrodes even in the mixed solution containing other proteins.

3.5 Detection of anti-HBcAg in human serum samples

The ability of the immunosensor to detect anti-HBcAg in real human serum solution was evaluated by the incubation of HBcAg-functionalized electrode with the anti-HBcAg ranging from 3.91 ng mL^{-1} to 125.00 ng mL^{-1} spiked in 1:1000 diluted human serum. The result was then compared with the detection of anti-HBcAg in a pure anti-HBcAg solution.

Figure 5(A) shows the impedimetric spectra of proposed immunosensor in 5 mM $K_3Fe(CN_6)$ and 0.1 M KCl after the incubation of HBcAg-functionalized electrode in the diluted serum containing designated anti-HBcAg concentration for two hours. As expected, the R_{ct} increases along the increment of concentration of anti-HBcAg in a mixed solution. The corresponding calibration curve (Figure 5(B)) clearly indicates the linearity relationship of both measured R_{ct} and the concentration of anti-HBcAg over a range of 3.91 ng mL^{-1} to 125.00 ng mL^{-1} with a linear regression equation of ΔR_{ct} = 0.0345[anti-HBcAg] + 6.467 and regression coefficient of 0.961.

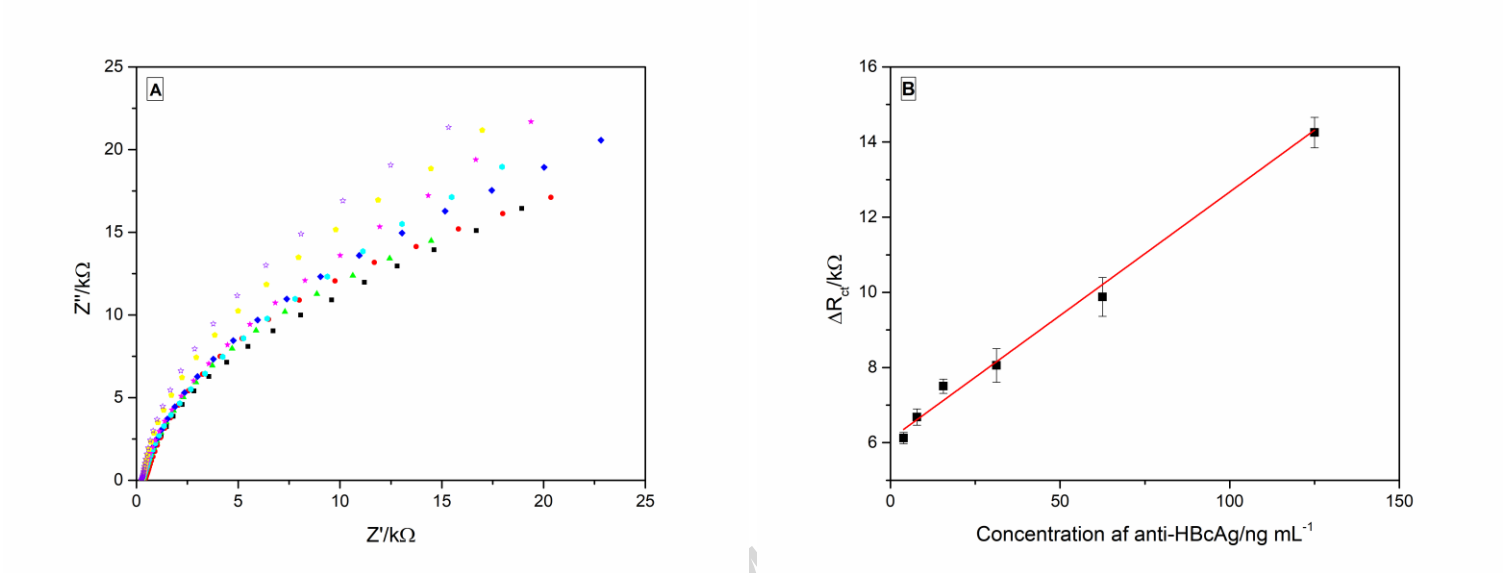

Figure 5: Impedimetric profile of HBcAg-functionalized electrode showing the detection of anti-HBcAg from diluted human serum. Nyquist plot of impedimetric analysis in 5 mM $K_3Fe(CN_6)$ and 0.1 M KCl (A), calibration curve showing relationship of ΔR_{ct} (changes in resistance after immunocomplex formation) and the varying concentration of anti-HBcAg in diluted human serum solution incubated on HBcAg-functionalized electrode (B). HBcAg-functionalized SPE (black square), and HBcAg-functionalized SPE that was incubated with unspiked serum (negative control) (red circle), 3.91 ng mL^{-1} anti-HBcAg in diluted serum (green triangle), 7.81 ng mL^{-1} anti-HBcAg in diluted serum (blue diamond), 15.63 ng mL^{-1} anti-HBcAg in diluted serum (cyan haxagon), 31.25 ng mL^{-1} anti-HBcAg in diluted serum (magenta star), 61.25 ng mL^{-1} anti-HBcAg in diluted serum (yellow pentagon), and 125.00 ng mL^{-1} anti-HBcAg in diluted serum (violet hollow star).

Based on the result obtained, the immunosensor was able to detect the anti-HBcAg within the concentration of 3.91 ng mL^{-1} to 125.00 ng $mL^{-}1$, with LOD of 5.60 ng mL^{-1} at 3 σ m^{-1}. There is 17.77% increment of Rct compared to SPE/rGO-en-AuNPs/HBcAg/BSA in the case of unspiked serum, and this might be contributed by the non-specific binding of some protein inside the serum to the HBcAg-functionalized surface [40].The value of RSD for each R_{ct} produced was calculated to compare between the R_{ct} produced by detection of pure anti-HBcAg (as in 3.2 Impedimetric detection of anti-HBcAg) and anti-HBcAg in the diluted human serum solution in order to evaluate the accurateness and precision of R_{ct} produced to detect anti-HBcAg in the diluted human serum solution. It was found that RSD values to be 1.99 %, 0.57 %, 0.54 %, 4.59 %, 6.71 % and 6.90 % for the comparison between 3.91 ng mL^{-1}, 7.81 ng mL^{-1}, 15.63 ng mL^{-1}, 31.25 ng mL^{-1}, 62.50 ng mL^{-1}, and 125.00 ng mL^{-1} of pure anti-HBcAg and anti-HBcAg in the diluted human serum. It was discovered that the HBcAg-functionalized electrodes detected efficiently the anti-HBcAg in the diluted human serum solution.

4. Conclusion

A protein-based antigen-functionalized SPE using rGO-en-AuNPs nanocomposite targeting anti-HBcAg was developed. This anti-HBcAg immunosensor is able to detect anti-HBcAg within clinically significant levels. Anti-HBcAg is a serological marker which indicates the exposure of an individual to HBV. Hence, one of the potential applications of this sensor is for the blood screening of anti-HBcAg prior to blood transfusion or organ transplantation to healthy recipients. Since the usage of SPE is on a disposable basis, this anti-HBcAg sensor will ease the clinical routine for anti-HBcAg screening as there will be no need for cleaning the electrode. This label-free anti-HBcAg immunosensor employed the immunoaffinity concept for an enhanced sensitivity and specificity for the biorecognition of anti-HBcAg. In addition, further miniaturization work for the development of a total integrated system is possible in view of the chosen method of electrochemistry.

Acknowledgements

This research was supported financially by Graduate Research Fellowship and Putra Graduate Initiative research grant scheme provided by Universiti Putra Malaysia, and Fundamental Research Grant Scheme provided by Ministry of Higher Education Malaysia.

REFERENCES

[1] J.M. Willey, L.M. Sherwood, C.J. Woolverton, Human disease caused by viruses and prions, in: Prescott's Microbiol., 8th Ed., McGraw-Hill, New York, NY, 2011: pp. 919–920.

[2] W.S. Tan, K.L. Ho, Phage display creates innovative applications to combat hepatitis B virus, World J. Gastroenterol. 20 (2014) 11650. doi:10.3748/wjg.v20.i33.11650.

[3] W.S. Tan, Fighting the Hepatitis B Virus: Past, Present & Future, Universiti Putra Malaysia Press, Serdang, 2016.

[4] C.W. Shepard, E.P. Simard, L. Finelli, A.E. Fiore, B.P. Bell, Hepatitis B Virus Infection : Epidemiology and Vaccination, Epidemiol. Rev. 28 (2006) 112–125. doi:10.1093/epirev/mxj009.

[5] J.F. Perz, G.L. Armstrong, L.A. Farrington, Y.J.F. Hutin, B.P. Bell, The contributions of hepatitis B virus and hepatitis C virus infections to cirrhosis and primary liver cancer worldwide, J. Hepatol. 45 (2006) 529–538. doi:10.1016/j.jhep.2006.05.013.

[6] H. Badrawy, R. Bakry, Anti-HBc and HBV-DNA detection in blood donors negative for hepatitis B virus surface antigen, Am. J. Mol. Biol. 3 (2013) 62–66. doi:10.4236/ajmb.2013.31008.

[7] R. Dickson, J. Everhart, J. Lake, Y. Wei, E. Seaberg, R. Wiesner, R. Zetterman, T. Pruett, M. Ishitani, J. Hoofnagle, Transmission of hepatitis B by transplantation of livers from donors positive for antibody to hepatitis B core antigen. The National Institute of Diabetes and Digestive and Kidney Diseases Liver Transplantation Database, Gastroenterology. 113 (1997) 1668–1674. doi:10.1053/gast.1997.v113.pm9352871.

[8] A. Hatzakis, E. Magiorkinis, C. Haida, HBV virological assessment, J. Hepatol. 44 (2006) S71–S76. doi:10.1016/j.jhep.2005.11.017.

[9] D. Milich, A. McLachlan, The nucleocapsid of hepatitis B virus is both a T-cell-independent and a T-cell-dependent antigen, Science (80-.). 234 (1986) 1398–1401. doi:10.1126/science.3491425.

[10] Q. Yuan, L.-W. Song, D. Cavallone, F. Moriconi, B. Cherubini, P. Colombatto, F. Oliveri, B.A. Coco, G. Ricco, F. Bonino, J.W.K. Shih, N.-S. Xia, M.R. Brunetto, Total Hepatitis B Core Antigen Antibody, a Quantitative Non-Invasive Marker of Hepatitis B Virus Induced Liver Disease, PLoS One. 10 (2015) e0130209. doi:10.1371/journal.pone.0130209.

[11] D.G.A. Cabral, E.C.S. Lima, P. Moura, R.F. Dutra, A label-free electrochemical

immunosensor for hepatitis B based on hyaluronic acid – carbon nanotube hybrid film, Talanta. 148 (2015) 209–215. doi:10.1016/j.talanta.2015.10.083.

[12] W.H. Gerlich, W. Lüer, Selective detection of IgM-antibody against core antigen of the hepatitis B virus by a modified enzyme immune assay, J. Med. Virol. 4 (1979) 227–238. doi:10.1002/jmv.1890040308.

[13] S.A. Lim, M.U. Ahmed, Electrochemical immunosensors and their recent nanomaterial-based signal amplification strategies: a review, RSC Adv. 6 (2016) 24995–25014. doi:10.1039/C6RA00333H.

[14] C. Kokkinos, A. Economou, M.I. Prodromidis, Electrochemical immunosensors: Critical survey of different architectures and transduction strategies, TrAC Trends Anal. Chem. 79 (2016) 88–105. doi:10.1016/j.trac.2015.11.020.

[15] R. Laocharoensuk, Development of Electrochemical Immunosensors towards Point-of-care Cancer Diagnostics: Clinically Relevant Studies, Electroanalysis. 28 (2016) 1716–1729. doi:10.1002/elan.201600248.

[16] X. Pei, B. Zhang, J. Tang, B. Liu, W. Lai, D. Tang, Sandwich-type immunosensors and immunoassays exploiting nanostructure labels: A review, Anal. Chim. Acta. 758 (2013) 1–18. doi:10.1016/j.aca.2012.10.060.

[17] S.A. Lim, H. Yoshikawa, E. Tamiya, H.M. Yasin, M.U. Ahmed, A highly sensitive gold nanoparticle bioprobe based electrochemical immunosensor using screen printed graphene biochip, RSC Adv. 4 (2014) 58460–58466. doi:10.1039/C4RA11066H.

[18] C. Kokkinos, A. Economou, P.S. Petrou, S.E. Kakabakos, Microfabricated tin-film electrodes for protein and DNA sensing based on stripping voltammetric detection of Cd(II) released from quantum dots labels, Anal. Chem. 85 (2013) 10686–10691. doi:10.1021/ac402783t.

[19] S. Li, H. Cui, Q. Yuan, J. Wu, A. Wadhwa, S. Eda, H. Jiang, AC electrokinetics-enhanced capacitive immunosensor for point-of-care serodiagnosis of infectious diseases, Biosens. Bioelectron. 51 (2014) 437–443. doi:10.1016/j.bios.2013.08.016.

[20] R.E. Ionescu, C. Gondran, L. Bouffier, N. Jaffrezic-Renault, C. Martelet, S. Cosnier, Label-free impedimetric immunosensor for sensitive detection of atrazine, Electrochim. Acta. 55 (2010) 6228–6232. doi:10.1016/j.electacta.2009.11.029.

[21] A. de la Escosura-Muñiz, M. Maltez-da Costa, C. Sánchez-Espinel, B. Díaz-Freitas, J. Fernández-Suarez, Á. González-Fernández, A. Merkoçi, Gold nanoparticle-based electrochemical magnetoimmunosensor for rapid detection of anti-hepatitis B virus antibodies in human serum, Biosens. Bioelectron. 26 (2010) 1710–1714. doi:10.1016/j.bios.2010.07.069.

[22] M.N. Omar, A.B. Salleh, N.L. Hong, A. Ahmad Tajudin, H.N. Lim, A. Ahmad Tajudin, Electrochemical detection of uric acid via uricase-immobilized graphene

oxide, Anal. Biochem. 509 (2016) 135–141. doi:10.1016/j.ab.2016.06.030.

[23] F.H. Cincotto, D.L.C. Golinelli, S.A.S. Machado, F.C. Moraes, Electrochemical sensor based on reduced graphene oxide modified with palladium nanoparticles for determination of desipramine in urine samples, Sensors Actuators B Chem. 239 (2017) 488–493. doi:10.1016/j.snb.2016.08.063.

[24] S. Stankovich, D.A. Dikin, G.H.B. Dommett, K.M. Kohlhaas, E.J. Zimney, E.A. Stach, R.D. Piner, S.T. Nguyen, R.S. Ruoff, Graphene-based composite materials, Nature. 442 (2006) 282–286. doi:10.1038/nature04969.

[25] C. Chan, J. Guo, C. Sun, M.-K. Tsang, F. Tian, J. Hao, S. Chen, M. Yang, A reduced graphene oxide-Au based electrochemical biosensor for ultrasensitive detection of enzymatic activity of botulinum neurotoxin A, Sensors Actuators B Chem. 220 (2015) 131–137. doi:10.1016/j.snb.2015.05.052.

[26] A. Benvidi, A.D. Firouzabadi, S.M. Moshtaghiun, M. Mazloum-Ardakani, M.D. Tezerjani, Ultrasensitive DNA sensor based on gold nanoparticles/reduced graphene oxide/glassy carbon electrode, Anal. Biochem. 484 (2015) 24–30. doi:10.1016/j.ab.2015.05.009.

[27] B. Dinesh, V. Veeramani, S.-M. Chen, R. Saraswathi, In situ electrochemical synthesis of reduced graphene oxide-cobalt oxide nanocomposite modified electrode for selective sensing of depression biomarker in the presence of ascorbic acid and dopamine, J. Electroanal. Chem. 786 (2017) 169–176. doi:10.1016/j.jelechem.2017.01.022.

[28] S. Singh, S.K. Tuteja, D. Sillu, A. Deep, C.R. Suri, Gold nanoparticles-reduced graphene oxide based electrochemical immunosensor for the cardiac biomarker myoglobin, Microchim. Acta. 183 (2016) 1729–1738. doi:10.1007/s00604-016-1803-x.

[29] M.H. Mat Zaid, J. Abdullah, N.A. Yusof, Y. Sulaiman, H. Wasoh, M.F. Md Noh, R. Issa, PNA biosensor based on reduced graphene oxide/water soluble quantum dots for the detection of Mycobacterium tuberculosis, Sensors Actuators B Chem. 241 (2017) 1024–1034. doi:10.1016/j.snb.2016.10.045.

[30] N. Shams, H.N. Lim, R. Hajian, N.A. Yusof, J. Abdullah, Y. Sulaiman, I. Ibrahim, N.M. Huang, Electrochemical sensor based on gold nanoparticles/ethylenediamine-reduced graphene oxide for trace determination of fenitrothion in water, R. Soc. Chem. 6 (2016) 89430–89439. doi:10.1039/C6RA13384C.

[31] W.S. Tan, M.R. Dyson, K. Murray, Hepatitis B Virus Core Antigen : Enhancement of Its Production in Escherichia coli , and Interaction of the Core Particles with the Viral Surface Antigen, Biol. Chem. 384 (2003) 363–371. https://www.degruyter.com/downloadpdf/j/bchm.2003.384.issue-3/bc.2003.042/bc.2003.042.xml.

[32] M.M. Bradford, A Rapid and Sensitive Method for the Quantitation Microgram Quantities of Protein Utilizing the Principle of Protein-Dye Binding, Anal. Biochem.

254 (1976) 248–254.

[33] D. Chen, M. Shen, Y. Cao, B. Bo, Z. Chen, Y. Shu, G. Li, Electrochemical identification of hepatocellular carcinoma based on the assay of human cervical cancer oncoprotein-1 in serum, Electrochem. Commun. 27 (2013) 38–41. doi:10.1016/j.elecom.2012.10.042.

[34] E. Arkan, R. Saber, Z. Karimi, M. Shamsipur, A novel antibody-antigen based impedimetric immunosensor for low level detection of HER2 in serum samples of breast cancer patients via modification of a gold nanoparticles decorated multiwall carbon nanotube-ionic liquid electrode, Anal. Chim. Acta. 874 (2015) 66–74. doi:10.1016/j.aca.2015.03.022.

[35] B. Khalilzadeh, N. Shadjou, H. Afsharan, M. Eskandani, H. Nozad Charoudeh, M.-R. Rashidi, Reduced graphene oxide decorated with gold nanoparticle as signal amplification element on ultra-sensitive electrochemiluminescence determination of caspase-3 activity and apoptosis using peptide based biosensor, Bioimpacts. 6 (2016) 135–147. doi:10.15171/bi.2016.20.

[36] J. Daniels, N. Pourmand, Label-Free Impedance Biosensors: Opportunities and Challenges, Electroanalysis. 19 (2007) 1239–1257. doi:10.1002/elan.200603855.

[37] Y. Xiao, S.N. Isaacs, Enzyme-linked immunosorbent assay (ELISA) and blocking with bovine serum albumin (BSA) - not all BSAs are alike, J. Immunol. Methods. 384 (2012) 148–151. doi:10.1016/j.jim.2012.06.009.

[38] G. Marcon, L. Messori, P. Orioli, M.A. Cinellu, G. Minghetti, Reactions of gold(III) complexes with serum albumin, Eur. J. Biochem. 270 (2003) 4655–4661. doi:10.1046/j.1432-1033.2003.03862.x.

[39] A. Syahir, K. Usui, K. Tomizaki, K. Kajikawa, H. Mihara, Label and Label-Free Detection Techniques for Protein Microarrays, Microarrays. 4 (2015) 228–244. doi:10.3390/microarrays4020228.

[40] A. Makaraviciute, A. Ramanavicius, A. Ramanaviciene, Development of a reusable protein G based SPR immunosensor for direct human growth hormone detection in real samples, Anal. Methods. 7 (2015) 9875–9884. doi:10.1039/C5AY01651G.

Graphical abstract